Proceedings of the 26th International Conference on Optical Fiber Sensors,
24–28 September 2018, Lausanne, Switzerland.
DOI:10.1364/OFS.2018.ThD4

Dual-channel OCT for Velocity Measurement in Microfluidic Channels

Evangelos Rigas, Jonathan M Hallam, Helen D Ford, Tom O H Charrett, Ralph P Tatam
Centre for Engineering Photonics, Cranfield University, Cranfield, Bedford, MK43 0AL, UK
r.p.tatam@cranfield.ac.uk

Abstract: A dual-beam Optical Coherence Tomography system has been developed, using a bespoke dual optical fibre, to simultaneously image microfluidic channel structures and measure high velocity flows (presently 250μm/s) from a single optical access point.
OCIS codes: 060.2370; 060.4230; 110.0110; 110.2350; 110.4155; 110.4500; 120.7250; 180.3170; 280.2490.

1. Introduction

Microfluidic chips are an increasing area of interest, used for "lab-on-a-chip" bio-analytical techniques, drug discovery, and chemical processing [1]. This requires optical, non-invasive flow-visualization techniques for characterising the flow across such chips. 3D micro particle image velocimetry (μPIV) using Confocal Microscopy is currently a favored technique, due to its multi-velocity-component capability and the sub-10 μm spatial resolution that can be achieved [2,3]; however, it requires optical access to the microfluidic chip from many directions making it difficult, or impractical, to implement in many cases. Doppler OCT [4], used for blood-flow measurement, has an angular dependence on velocity sensitivity which falls to zero for the convenient ninety-degree implementation, and thus also requires multiple access ports to measure 3D flows.

Optical Coherence Tomography (OCT) is capable of spatial resolution down to a few μm and depth resolution down to ~1μm [5,6], at ~30Hz for a ~2mm cross-section. When the target is a semi-transparent material, the sensing light penetrates to form an ~1mm deep image of sub-surface structures. OCT is a mature technique in the medical imaging field with instruments available from commercial providers and these systems have been applied for microfluidic flow tracking with limiting velocities ~1mm/s [7].

Here, a bespoke dual optical fibre has been designed and constructed, paired with an optimized bulk-optic sensor head, an advanced akinetic swept-source laser operating at 96kHz, and a custom built dual-channel OCT processing system. The instrumentation has been packaged as a prototype for use outside the optics laboratory. The use of the dual optical fibre allows detection of particles at velocities theoretically up to three orders of magnitude greater than previously possible using a single channel.

2. Experimental

The difficulty in measuring the velocity of fluidic flows using scanned-beam imaging techniques such as OCT is that the particles must be identifiably present in sequential image frames, either uniquely using particle tracking velocimetry techniques (PTV) or statistically using particle imaging velocimetry (PIV) techniques. Thus, the maximum particle velocity that can be detected is set by the OCT system imaging frame rate, itself typically limited by the maximum galvonometer scan rate.

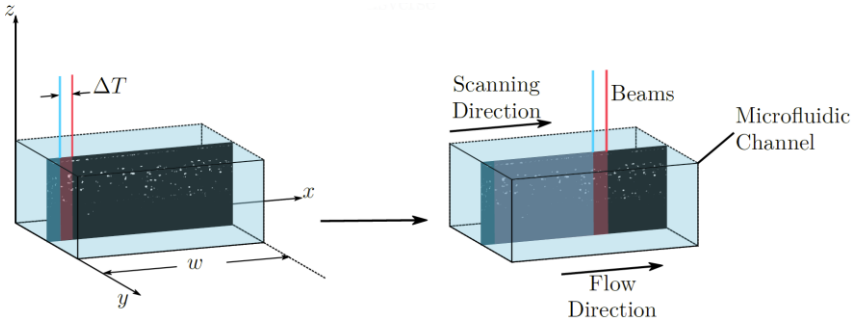

Fig. 1. Diagram of dual-channel OCT system imaging for particle flow velocity measurement. Both left-and-right figures show the volume of a microfluidic channel with a measured cross-sectional particle image within. The z-(axial), x-(lateral, in the direction of flow) and y-(lateral, across the flow) axes are shown. 'w' is the width of the scan, shown at the start on the left and partially completed on the right. The ΔT spatio-temporal separation between the beams is marked, as is the particle flow direction.

The dual-channel OCT approach outlined in figure 1 removes the scan-rate constraint, as the dual beams capture two frames simultaneously (analogous to double-exposure camera PIV techniques), albeit at a small physical offset ΔT determined by the magnification of the system and the separation of the dual optical fibre ends. Since the dual beams are scanned through space over time this physical offset can also be expressed as a time delay between the two beams; hence, smaller optical fibre end separation allows higher velocities to be accessed. Due to the interaction between the motion of the beams and the particle flow, scanning in the same direction as the flow improves velocity resolution but reduces the maximum measurable velocity; and scanning against the main flow direction degrades velocity resolution but increases the maximum measurable velocity.

The theoretical maximum detectable velocity is that required for a particle to be able to pass through the micrometre width of the beam without being detected by the kHz sweep of the laser; however, neither PTV or PIV techniques are presently capable of determining velocity with such sparse information.

The dual-channel OCT system schematic is shown in figure 2. It is driven by an Insight akinetic Swept-Source Laser delivering 9.16mW of power at a maximum sweep rate of 96kHz between 1526-1608nm with a flat-top power profile. This light is immediately split by a broadband single-mode coupler, propagated first through a pair of broadband circulators, then via the bespoke dual optical fibre to the OCT head unit. Light from the head unit retraces this path until directed by the circulator to a photodetector. Each optical fibre in the dual optical fibre head has its own circulator and photodetector and balanced detection is not used in this scheme. The bandwidth is limited by a passive electronic filter to 60MHz to reduce the detector noise. The data is captured at 500MS/s and 12-bit resolution using an Alazartech DAQ. Bespoke acquisition code allows direct recording of 4096 data points in each 96kHz A-scan to a solid-state drive for post-processing. In the initial data processing regions of instability in the akinetic laser wavelength sweep are removed by the application of a data valid vector. The remaining points associated with valid wavelengths are then windowed with a Blackman-Harris filter, and a fast-Fourier transform is performed to obtain each A-scan, each of which represents one of 600 columns in the OCT image.

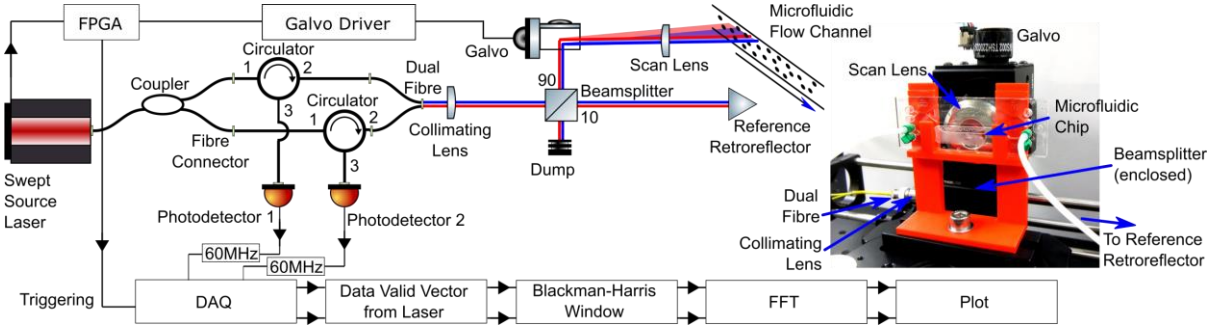

Fig. 2. Left: Schematic diagram of optical system including advanced akinetic swept-source laser; Alazartech dual-channel data acquisition card (DAQ) and immediate post-processing; packaged dual-channel OCT prototype comprising coupler, circulators, photodetectors, FPGA and galvo drivers; bespoke dual optical fibre; OCT sensing head comprising triplet collimating lens, 90:10 ratio beamsplitter, beam dump, galvos, OCT scan lens and reference retroreflector; and microfluidic flow channel. Right: Picture of sensing head and microfluidic chip.

Light is coupled into the OCT head via the bespoke dual optical fibre. The use of an FC/APC connector allows a robust and stable connection to be formed with an achromatic triplet collimating lens. The triplet collimator mount allowed for rotation so the bespoke dual optical fibre orientation can be aligned with the galvanometer scan as in figure 1. The light then propagates through free space to a 90% reflective beamsplitter cube. The 10% of light transmitted is directed to a retroreflector which serves as a reference mirror without requiring a focusing lens, and is insensitive to angular misalignment. All components are broadband antireflection coated. The microfluidic channel is imaged by the 90% of the input light reflected by the beamsplitter. X-and-Y directional steering of the beams is accomplished by a silvered galvanometer mirror system. This component limits the collimated beam diameter to 5mm. The beams are focused onto the microfluidic channel using an OCT scan lens with 18mm focal length. This creates a narrow beam waist for good lateral resolution, but limits the accessible Depth of Field, consistent with the literature [8].

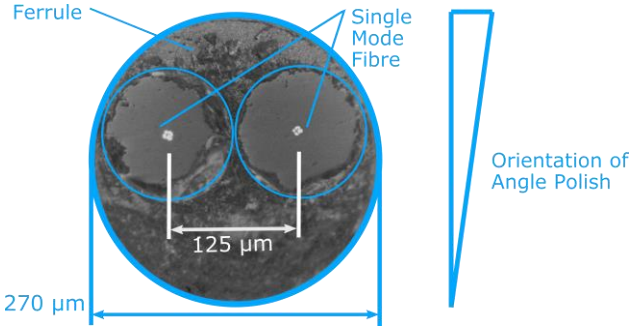

Fig. 3. Bespoke dual optical fibre, shown imaged end-on using an optical microscope. The optical cores of the 1550nm single-mode optical fibres are illuminated from the far end using a green laser at which wavelength the exhibits multimode behaviour in the fibre. The orientation of the angle polish is indicated, with the microscope focus being at the core of the optical fibres.

The beam waists were 8µm for beam A and 11µm for beam B, separated by a lateral distance of 550µm and a z-(axial) distance of 60µm, with a Rayleigh Range of 150µm. This was determined by incrementally occluding each beam using a razor-blade edge, mounted on a micrometre-accurate X-and-Y positioning stage. Comparing the known 125µm separation of the dual optical fibre with the lateral separation of the beam waists implies a

magnification of x4.4; however, both the angular separation of the beams, and the z-axis separation between the focal points imply that some of this separation is due to divergence between the two beams. This is likely because the two beams are perforce off-centre with respect to the small lenses of the triplet collimator.

The bespoke dual optical fibre was created by bonding two commercially available single-mode 1550nm telecommunication optical fibres into a single ceramic ferrule. The optical fibres had 9µm optical core diameter, 125µm cladding diameter, and the ferrule had an internal diameter of 270µm. This is shown imaged end-on using an optical microscope with the cores illuminated from the opposite end in figure 3, which confirmed the distance between the cores to be 125µm. The ferrule was then mounted in an FC/APC connector, which allowed angle-polishing using a commercial jig. The angle polish was performed across the optical fibre ends so that each optical fibre would be the same distance from the triplet collimating lens when mounted enabling both beams can be collimated simultaneously.

3. Results

A microfluidic reaction chip of 800µm channel depth was filled with 10µm latex particles in partial buffer solution glycerol suspension, density matched to the latex particles. This was imaged using the dual-channel OCT system, as shown in figure 4. The images from beam A and beam B have been offset by the measured separation of the two beams. Bright lines in both images represent the surface of the microfluidic chip, the top of the microfluidic channel within the chip, and the bottom of the microfluidic channel. The last of these appears somewhat less clearly because the light creating that image must make the round-trip pass through the channel and the light is obstructed by the particles, shadowing the region below.

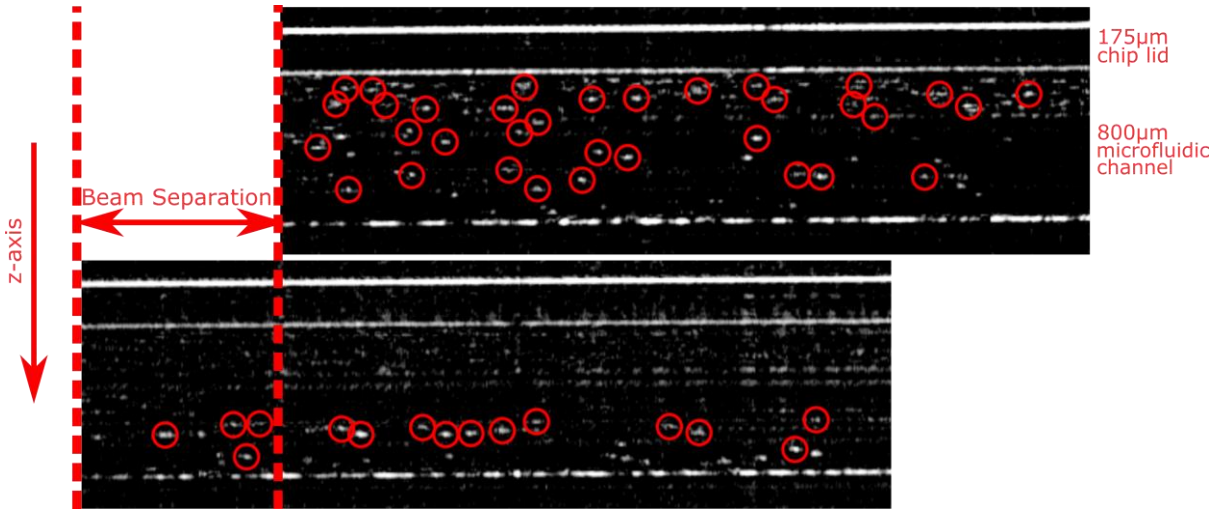

Fig. 4. Imaged 10µm particles in an 800µm deep microfluidic channel with a 175µm thick lid. The upper panel is generated by beam A, the lower panel by beam B. The algorithmically identified particles are circled in red, and channel features are annotated. The panels have been offset by the determined 550µm separation between the two beams after magnification by the dual-channel OCT system lenses. The physical separation between each core of the dual optical fibre is 125µm.

In this case, because of the offset in focal depth, relatively few coincident particles were identified by each beam (an effect previously reported [9]). Thus, it was not possible to track particles from beam A to beam B in sufficient numbers and with broad enough distribution through the depth of the microfluidic chip (on the z-axis) to generate a velocity profile; hence, the highest velocities theoretically measurable were not observed. Instead, a lower velocity flow was used, and the particles were tracked between sequential frames from each beam.

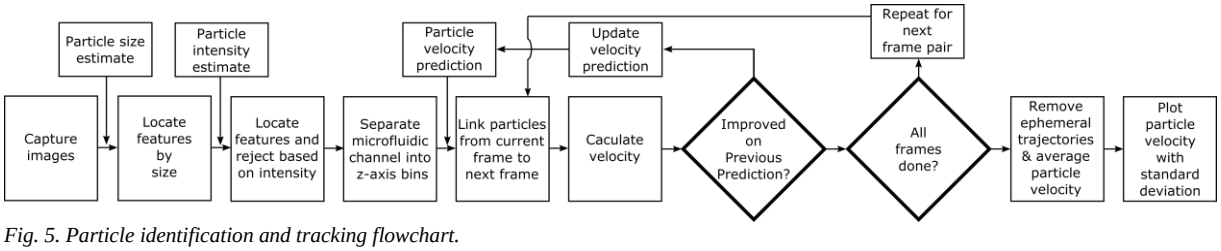

Fig. 5. Particle identification and tracking flowchart.

Particle tracking was performed using the open source Python library trackpy [10,11] using methodology as shown in figure 5. Initially, a particle intensity estimate is determined from a reference measurement. Particle tracking images are then captured, and features are located by intensity. A priori knowledge of particle size is used to reject features forming part of the microfluidic chip, especially those from the lower channel surface. The microfluidic channel is separated into bins along the z-axis, since Poiseuille flow is expected which depends

on distance from the channel walls. A non-critical velocity prediction is input and iteratively improved based on each sequential pair of frames to determine the measured particle velocity for each particle between each pair of frames. Finally, particles tracked for less than two pairs of frames are rejected to reduce the influence of spurious particle misidentification or tracking errors. The average velocity is calculated for each particle.

The individual particle velocities are then grouped into bins of the fifteen nearest particles on the z-axis (depth through channel), and the average position, velocity, and standard deviation from that velocity are determined (as shown in figure 6), which demonstrates Poiseuille flow, although the line of best fit does not fall to zero at the edges of the channel as expected. This is believed to be an artefact of variance in the pump pressure driving the flow, possibly caused by the ingress of air bubbles to the system; or, that the particles interacting directly with the microfluidic channel surfaces exhibit either slip or roll, allowing higher velocities throughout the channel. The identified particles cluster at the respective beam foci, and further from the beam foci the quality of the velocity information obtained degrades, as seen in the error bars for beam B.

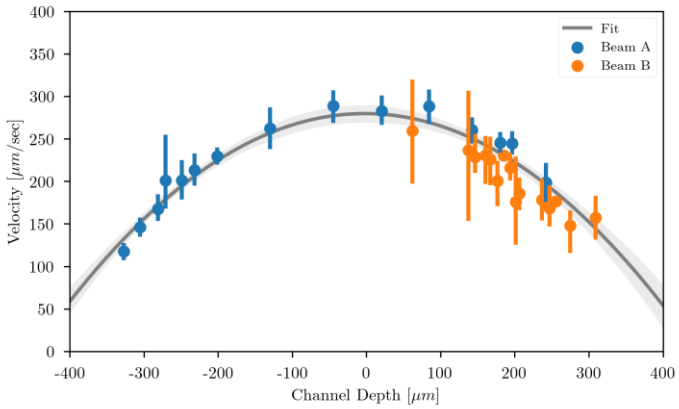

Fig. 6. Identified 10μm particles in an 800μm deep channel, their average velocities across all frames and the standard deviation from those velocities from frame-to-frame, plotted against their position from the center of the channel. A Poiseuille flow fit is shown in grey.

3. Conclusions and Discussion

A dual-channel OCT system has been developed for simultaneous imaging of microfluidic channel structures, and (particle seeded) high velocity flows through them, using a single optical access point. To achieve this a bespoke dual fibre optic has been developed together with a packaged dual-channel OCT prototype and an optimized OCT head. This together with the application of the open source trackpy particle tracking library, has been used to monitor microfluidic flows, and Poiseuille flow has been observed in an 800μm deep test chip.

It is anticipated that in the short-term the problem of tracking particles from beam A to beam B will be resolved, allowing access to the high velocity regime, in principle up to the meters-per-second regime. This should be achievable with improvements to the connection between the bespoke dual optical fibre and the OCT sensing head. The instrument can then be tested against a range of more featured flows, particularly exhibiting two-dimensional velocities, formed by slopes and corners in the microfluidic channels. Alternatively, for more turbulent flows requiring three-dimensional tracking, across-microfluidic channel scanning, or end-on scanning, could be investigated. For higher particle densities, particle imaging velocimetry, utilizing correlation based approaches rather than tracking, will be required. Further improvements to the dual optical fibre to reduce the spacing between the fibre cores should allow access to even higher velocity regimes.

4. References

[1] N. Shembekar, C. Chaipan, R. Utharala, C.A. Merten, *"Droplet-based microfluidics in drug discovery, transcriptomics and high-throughput molecular genetics"*, Lab Chip **16,** 1314-1331 (2016).

[2] C. Cierpka, C.J. Kahler, *"Particle imaging techniques for volumetric three-component (3D3C) velocity measurements in microfluidics"*, J Vis (Tokyo) **15**, 1-31 (2012).

[3] R. Lima, S. Wada, K. Tsubota, T. Yamaguchi, *"Confocal micro-PIV measurements of three-dimensional profiles of cell suspension flow in a square microchannel"*, Meas. Sci. Technol. **17,** 797-808 (2006).

[4] R.A. Leitgeb, R.M. Werkmeister, C. Blatter, L. Schmetterer, *"Doppler Optical Coherence Tomography"*, Prog Retin Eye Res. **41,** 26-43 (2014)

[5] L.S. Magwaza, H.D. Ford, P.J.R. Cronje, U.L. Opara, S. Landahl, R.P. Tatam, L.A. Terry, *"Application of optical coherence tomography to non-destructively characterise rind breakdown disorder of 'Nules Clementine' mandarins"*, Postharvest Biol. Technol. **84,** 16-21 (2013).

[6] H.D. Ford and R.P. Tatam, *"Passive OCT probe head for 3D duct inspection"*, Meas. Sci. Technol., **24,** 094001 (2013).

[7] S. Jonas, D. Bhattacharya, M.K. Khokha, M.A. Choma, *"Microfluidic characterization of cilia-driven fluid flow using optical coherence tomography-based particle tracking velocimetry"*, Biomed. Opt. Express **2,** 2022-2034 (2011).

[8] J.A. Izatt, M.A Choma, A. Dhalla, *"Theory of Optical Coherence Tomography"* in *Optical Coherence Tomography Technology and Applications 2nd edition* W. Drexler and J.G Fujimoto. ed. (SpringerReference, Switzerland, 2015).

[9] J. Holmes, *"Theory and applications of multi-beam OCT"*, Proc. SPIE 7139 (2008).

[10] D. Allan, T. Caswell, N. Keim and C. van der Wel,, *trackpy: Trackpy v0.3.2*, 19th August 2016.

[11] J.C. Crocker, D.G. Grier, *"Methods of Digital Video Microscopy for Colloidal Studies"*, J. Colloid Interface Sci. **179,** 298-310 (1996).

Dual-channel OCT for velocity measurement in microfluidic channels.

Rigas, Evangelos

2018-09-28

Rigas E, Hallam J, Ford H, et al., Dual-channel OCT for velocity measurement in microfluidic channels. 26th International Conference on Optical Fiber Sensors, 24–28 September 2018, Lausanne, Switzerland.

https://doi.org/10.1364/OFS.2018.ThD4